Proceedings of Papers – 5th International Conference on Electrical, Electronic and Computing Engineering, IcETRAN 2018, Palić, Serbia, June 11 – 14, 2018 ISBN 978-86-7466-752-1

Kinematic Parameters for Generation of Acceleration Force Profile of a Centrifuge Flight Simulator

Vladimir Kvrgic, Jelena Vidakovic

***Abstract*—Pilots of modern combat aircrafts are exposed to the devastating effects of high acceleration forces. The pilots' ability to perform tasks under these extreme flight conditions must be examined. For the purpose of pilot training, a centrifuge flight simulator for pilot training is designed as a 3DoF manipulator with rotational axes. Through rotations about these axes, acceleration forces that act on the aircraft pilots are simulated. The centrifuge flight simulator must achieve velocity, acceleration and acceleration rates (jerks) of the pilot through rotation of its arm. A constant increase/decrease in the acceleration force acting on a pilot is required according to specifications. To prevent the abrupt change in the arm angular velocity before and after the desired linear change in the acceleration force, smoothing of the acceleration force profile through arm motion is necessary. The roll and pitch angles (the angles of the second and the third link) and the arm angular velocity define the orthogonal components of the resultant vector of the acceleration force that are experienced by the simulator pilot. The determination the arm angular velocity and angular acceleration profiles and the roll and pitch angles needed for achieving the desired acceleration force components of the centrifuge flight simulator is presented in this paper.**

***Index Terms*—Centrifuge flight simulator, Acceleration force profile, Roll and pitch angles**

I. INTRODUCTION

Modern thrust-vectored jet aircraft have the capability of developing multi-axis accelerations, especially during the performance of "super-manoeuvres" [1-3]. These "agile" aircraft are capable of unconventional flight with high angles of attack, high agile motions with thrust-vectored propulsion in all 3 aircraft axes, rotations around those axes and acceleration forces of up to G = 9 g (g is Earth's acceleration), with acceleration rates (jerk) of up to dG/dt = 9 g/s [4,5]. The connection between the jerk and the movements of the human body is shown in [6–10]. Hence, the destructive effects of the high acceleration forces and the rapid changes of these forces on the pilot's physiology and the ability to perform tasks under these flight conditions must be tested. A human centrifuge is used for the reliable generation of high G onset and offset rates and high levels of sustained G, to test the reactions and the tolerances of the pilots. Within aerospace engineering, an acceleration force $G=a/\mathrm{g}$, $a=(a_n^2+a_t^2+\mathrm{g}^2)^{1/2}$ is the magnitude of the total acceleration acting on the pilot. It correlates with total inertial effects experienced by the simulator pilot; a_n is normal, and a_t is tangential acceleration. G force is dimensionless, but, it is typically expressed in unit of "g." Thus, an acceleration a of, for example, 98.1 m/s^2 is given with G = 10 g.

The centrifuge (Fig. 1) has the form of a three degree-of-freedom (3DoF) manipulator with rotational axes, where the pilot's head (or chest for some of the training) is considered to be the end-effector [11,12,13]. The arm rotation around the vertical (planetary) axis is the main motion that achieves the desired acceleration force. The centrifuge flight simulator (CFS) must achieve velocity, acceleration and jerk of the pilot through suitable rotations of the centrifuge arm about this axis. The arm carries a gimballed gondola system, with two rotational axes providing pitch and roll capabilities. The roll axis lies in the plane of the arm rotation, perpendicular to the main rotational axis, i.e., in the x-axis direction. The pitch (y) axis is perpendicular to the roll axis. A similar centrifuge, driven by three hydraulic actuators, is described in [15]. In [16,17], another realisation of the centrifuge is described. Its second axis is perpendicular to the first axis and is along the horizontal line when the centrifuge is in a neutral position. The task of the roll and pitch axes is to direct the acceleration force into the desired direction. It is considered that the pilot's head (chest) is placed in the intersection of the gondola's roll and pitch axes. In this way, the centrifuge produces the transverse G_x, lateral G_y and longitudinal G_z acceleration forces and the roll $\hat{\omega}_x$, pitch $\hat{\omega}_y$ and yaw $\hat{\omega}_z$ angular velocities to simulate the aircraft's acceleration forces and angular velocities. Fig. 2 shows these acceleration force G components. The three main axes of the coordinate frame attached to the human body are: the x axis, which extends from the face to the back, the y axis, which extends from the pilot's right to the pilot's left side, and the z axis, which extends from the head to the pelvis.

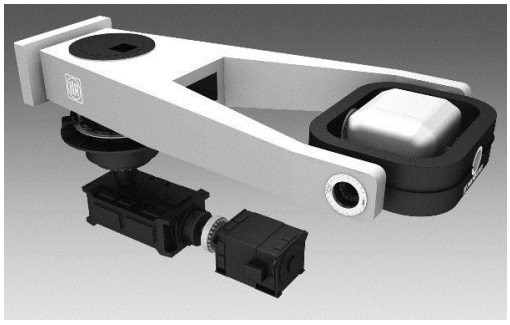

Fig. 1. Centrifuge with 3 degrees of freedom.

Vladimir Kvrgic is with the University of Belgrade, Institute Mihajlo Pupin (IMP), Volgina 15, 11060 Belgrade, Serbia, vladimir.kvrgic@pupin.rs.

Jelena Vidakovic is with Lola Institute, Kneza Viseslava 70a, 11030 Belgrade, Serbia, jelena.vidakovic@li.rs.

The presented CFS is aimed not only at improving $+G_z$ tolerance but also at the combined G_y/G_z and G_x/G_z exposure. Multi-axis sustained accelerations can either enhance or reduce the $+G_z$ tolerance of the pilot, depending on the direction of the net gravitoinertial force. G_y acceleration in conjunction with G_z acceleration can enhance G tolerance. G_x acceleration in addition to G_z acceleration can reduce the G tolerance [3].

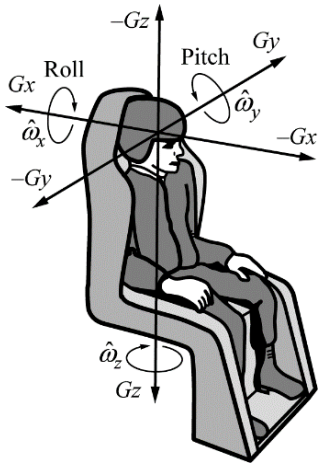

Fig. 2. The transverse, lateral and longitudinal acceleration force components G_x, G_y and G_z, which act on the pilot in the simulator.

Although the centrifuge is capable of generating acceleration forces of up to 15 g for materials testing purposes, forces that are less than or equal to 9 g are used for pilot training.

Reference [13] shows a control algorithm which includes a simulation of the inertial loads that were exerted on the pilot during flight. This approach allows for virtual centrifuge prototyping and analysis of the interaction between the engine control, the simulation of inertial forces acting on the pilot and the structure of the centrifuge. A similar algorithm for a spatial disorientation trainer is presented in [14]. A virtual simulator of the CFS, used for testing and verification of presented control algorithms, is described in [18].

The calculation of the acceleration forces that act on the pilot in the gondola and required link angles for the second and the third axis of the centrifuge is given in Section II. Calculation of the angular acceleration of the centrifuge arm $\ddot{q}_1$, the smoothing of acceleration force G profile and the control algorithm of the centrifuge movement are given in Section III. Verification of the results obtained using the proposed control algorithm is presented in Section IV. Finally, concluding remarks are given in Section V.

II. Acceleration Force Components and Roll and Pitch Link Angles

A. Forward kinematics of the centrifuge

The coordinate frames for the centrifuge links are depicted on Fig. 3. The base is denoted by 0, the arm by 1 (arm length a_1=8 m), the roll ring by 2 and the gondola by 3. The arm rotation angle is denoted by $q_1=\psi$, the roll ring rotation angle by $q_2=\phi$ and the gondola rotation angle (pitch) by $q_3=\theta$. The roll axis rotation range is ±180° and the pitch axis rotation range is ±360°. The centrifuge base coordinates are denoted by $x_0y_0z_0$, the arm coordinates by $x_1y_1z_1$ (link 1), the roll ring coordinates by $x_2y_2z_2$ (link 2), the gondola coordinates by $x_3y_3z_3$ (link 3) and the pilot coordinates by xyz. Here, $x_3=x$, $y_3=y$ and $z_3=z$. The homogenous transformation matrices (HTM) for the relation between the centrifuge link coordinate frames are as follows:

$$ {}^0\mathbf{T}_1=\begin{bmatrix} c_1 & 0 & s_1 & a_1c_1 \\ s_1 & 0 & -c_1 & a_1s_1 \\ 0 & 1 & 0 & 0 \\ 0 & 0 & 0 & 1 \end{bmatrix},\ {}^1\mathbf{T}_2=\begin{bmatrix} -s_2 & 0 & c_2 & 0 \\ c_2 & 0 & s_2 & 0 \\ 0 & 1 & 0 & 0 \\ 0 & 0 & 0 & 1 \end{bmatrix},\ {}^2\mathbf{T}_3=\begin{bmatrix} -s_3 & 0 & -c_3 & 0 \\ c_3 & 0 & -s_3 & 0 \\ 0 & -1 & 0 & 0 \\ 0 & 0 & 0 & 1 \end{bmatrix} \quad (1) $$

Herein the convenient shorthand notation, $\sin(q_i)=s_i$, $\cos(q_i)=c_i$, i=1,2,3 is used. The forward kinematics that is related to the robot geometry is used to calculate the position and orientation of the links and end-effector (in this case, the pilot's head/chest) with respect to the centrifuge variables q_1, q_2 and q_3. It is determined from the following matrices:

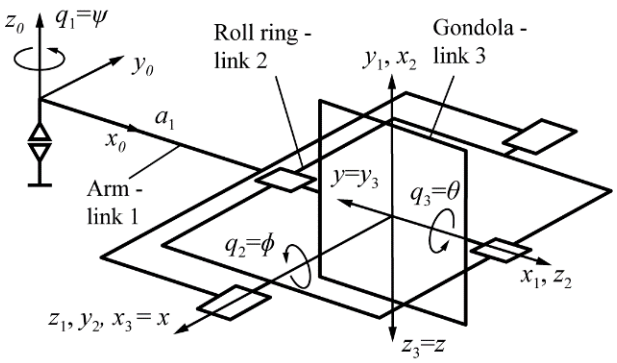

Fig. 3. Coordinate frames of the 3-axis centrifuge links.

$$ {}^0\mathbf{T}_2=\begin{bmatrix} -c_1s_2 & s_1 & c_1c_2 & a_1c_1 \\ -s_1s_2 & -c_1 & s_1c_2 & a_1s_1 \\ c_2 & 0 & s_2 & 0 \\ 0 & 0 & 0 & 1 \end{bmatrix} \quad (2) $$

$$ {}^0\mathbf{T}_3=\begin{bmatrix} c_1s_2s_3+s_1c_3 & -c_1c_2 & c_1s_2c_3-s_1s_3 & a_1c_1 \\ s_1s_2s_3-c_1c_3 & -s_1c_2 & s_1s_2c_3+c_1s_3 & a_1s_1 \\ -c_2s_3 & -s_2 & -c_2c_3 & 0 \\ 0 & 0 & 0 & 1 \end{bmatrix} \quad (3) $$

B. Calculation of the simulator pilot acceleration force components

Fig. 4 shows coordinate frames, angles, angular velocities and acceleration forces of the centrifuge.

The linear acceleration experienced by the simulator pilot at the intersection point of the roll and pitch axes is:

$$ \dot{\mathbf{v}}_1=\dot{\mathbf{v}}_2=\dot{\mathbf{v}}_3=\begin{bmatrix} \dot{v}_{1x} & \dot{v}_{1y} & \dot{v}_{1z} \end{bmatrix}^T=a_1\begin{bmatrix} s_1\dot{\omega}_1+c_1\omega_1^2 & c_1\dot{\omega}_1-s_1\omega_1^2 & 0 \end{bmatrix}^T \quad (4) $$

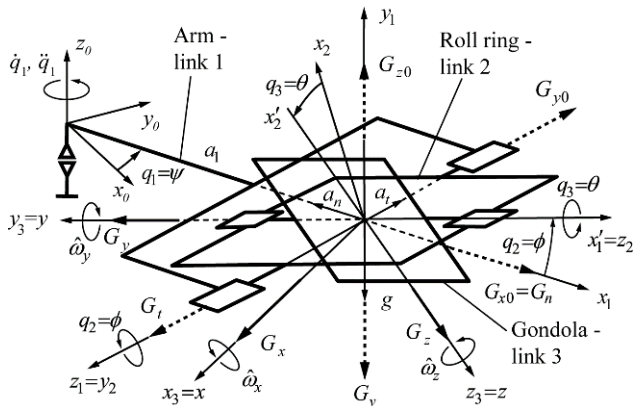

Fig. 4. Coordinate frames, angles, angular velocities and acceleration forces of the centrifuge.

Based on (4) for q_1=0 and adding the gravitational acceleration g, the orthogonal components G_n, G_t and G_v for the normal (radial), tangential and vertical acceleration force G components, respectively, that are experienced by the simulator pilot are the following:

$$\begin{bmatrix} G_{x0} \\ G_{y0} \\ G_{z0} \end{bmatrix} = \frac{1}{g}\begin{bmatrix} -a_n \\ a_t \\ -g \end{bmatrix} = \begin{bmatrix} a_1\omega_1^2/g \\ -a_1\dot{\omega}_1/g \\ -1 \end{bmatrix} = \begin{bmatrix} G_n \\ -G_t \\ -G_v \end{bmatrix} \tag{5}$$

The link angles $q_2=\phi$ and $q_3=\theta$ and the angular velocity $\dot{q}_1$ of the arm define the orthogonal components G_x, G_y and G_z of the resultant vector **G** that are experienced by the simulator pilot. Based on (3) and (5), the resultant vector **G** is:

$$\mathbf{G}=\begin{bmatrix} G_x & G_y & G_z \end{bmatrix}^T = \mathbf{D}_3^{-1}\begin{bmatrix} G_{x0} & G_{y0} & G_{z0} \end{bmatrix}^T \tag{6}$$

$$G_x = s_3(G_{x0}s_2+c_2)-G_{y0}c_3 \tag{7}$$

$$G_y = -G_{x0}c_2+s_2 \tag{8}$$

$$G_z = c_3(G_{x0}s_2+c_2)+G_{y0}s_3 \tag{9}$$

Matrix $\mathbf{D}_3$ in (6) is the rotational matrix part of (3). Angles $q_1=\psi$, $q_2=\phi$ and $q_3=\theta$ and their derivatives define the roll, pitch and yaw angular velocities of $\hat{\omega}_x$, $\hat{\omega}_y$ and $\hat{\omega}_z$, which are experienced by the simulator pilot; they are given as follows (for q_1=0):

$$\hat{\boldsymbol{\omega}}=\begin{bmatrix} \hat{\omega}_x \\ \hat{\omega}_y \\ \hat{\omega}_z \end{bmatrix} = \mathbf{D}_3^{-1}\boldsymbol{\omega}_3 = \begin{bmatrix} \dot{q}_2c_3-\dot{q}_1c_2s_3 \\ -\dot{q}_3-\dot{q}_1s_2 \\ -\dot{q}_2s_3-\dot{q}_1c_2c_3 \end{bmatrix} \tag{10}$$

C. Calculation of the centrifuge roll and pitch angles

The centrifuge roll angle is calculated by (8), which uses the given lateral force G_y, in the following way:

$$q_2=\phi=\text{atan}\,2(G_{x0}+G_y(1-G_y^2+G_{x0}^2)^{1/2},1-G_y^2) \tag{11}$$

If $G_y<0$ and $G_y^2>1$, then $q_2=q_2+\pi$. The roll angle can be calculated only if $G_{x0}^2+1\geq G_y^2$. Otherwise, it is not possible to achieve the given lateral force G_y. For G_y=0, (11) yields:

$$q_2=\phi=\text{atan}\,2(G_{x0},1) \tag{12}$$

Equations (7) and (9) show that it is not possible to achieve both of the given G_x and G_z forces, even when they are in the allowed ranges. As a result, the centrifuge pitch angle is calculated by (7), using the given transverse force G_x, or by (9), using the given longitudinal G_z force. Equation (7) yields:

$$q_3=\theta=\text{atan}\,2(G_{y0}b+G_x(b^2+G_{y0}^2-G_x^2)^{1/2},b^2-G_x^2) \tag{13}$$

where $b=G_{x0}s_2+c_2$. If $b^2+G_{y0}^2<G_x^2$, then it is not possible to achieve the given transverse force G_x. For G_x=0, (12) yields:

$$q_3=\theta=\text{atan}\,2(G_{y0},b) \tag{14}$$

Equation (9) yields the following:

$$q_3=\theta=\text{atan}\,2(G_{y0}d-G_z(b^2+G_{y0}^2-G_z^2)^{1/2},G_z^2-G_{y0}^2) \tag{15}$$

If $G_z<0$ and $G_z^2>G_{y0}^2$, then is $q_3=q_3-\pi$. If $b^2+G_{y0}^2<G_z^2$, then it is not possible to achieve the given longitudinal G_z force. Basic pilot training implies that $G_z=G$ (G_x=0 and G_y=0). As a result, the roll and pitch angles are given by (12) and (14).

III. The Control Algorithm of the Centrifuge Movement

A. Calculation of the arm angular acceleration $\ddot{q}_1$

Equation (5) gives the resulting acceleration force that is experienced by the simulator pilot at the intersection point of the roll and pitch axes (herein q_1=0 for simplicity, because G does not depend on the position of the CFS arm) as a function of the angular velocity and acceleration of the centrifuge arm, which is:

$$G=(G_{x0}^2+G_{y0}^2+G_{z0}^2)^{1/2}$$

$$=\frac{1}{g}(a_n^2+a_t^2+g^2)^{1/2}=\frac{1}{g}[a_1^2(\dot{q}_1^4+\ddot{q}_1^2)+g^2]^{1/2} \tag{16}$$

According to the requirement that the increase in the acceleration force G should be constant and equal to n_d, the following is valid: $dG/dt=n_d$, which yields $d([a_1^2(\dot{q}_1^4+\ddot{q}_1^2)+g^2]^{1/2})=n_d\,g\,dt$. If we assign the resulting

acceleration with $a = G\,\mathrm{g}$, then the previous equation will be:

$$da = d([a_1^2(\dot{q}_1^4 + \ddot{q}_1^2) + \mathrm{g}^2]^{1/2}) = n_d\,\mathrm{g}\,dt \qquad (17)$$

The previous differential equation does not have a solution in closed form.

In each interpolation period, the robot controller determines a constant angular velocity of each motor link. An interpolation period of Δt=0.005 s is adopted here. During this period, the servo system of the controller compares (every 0.001 s) the given and achieved motor rotor positions and corrects rotor angular velocities with the aim of keeping them constant within this period. Based on these observations, an approximated solution from (17) using a discretisation technique is obtained in the following manner. Differential equation (17) is solved for each interpolation period Δt. For the desired rate of change of acceleration $\Delta a/\Delta t = n_d\,\mathrm{g}$, the acceleration a will first be calculated on the basis of this acceleration in the previous interpolation period, a_{prev}, in the following way:

$$a = a_{prev} + \Delta a\,,\ \Delta a = n_d\,\mathrm{g}\,\Delta t \qquad (18)$$

If we assign the angular velocity of the centrifuge arm in the previous interpolation period with $\dot{q}_{1prev}$, we obtain:

$$\dot{q}_1 = \dot{q}_{1prev} + \ddot{q}_1\,\Delta t \qquad (19)$$

If we substitute $\dot{q}_1$, calculated in this manner, into the equation $a^2 = a_1^2\dot{q}_1^4 + a_1^2\ddot{q}_1^2 + \mathrm{g}^2$ and neglect the terms with Δt^3 and Δt^4, the following equation for calculating the centrifuge arm acceleration is obtained:

$$\ddot{q}_1 = \frac{-2\dot{q}_{1prev}^3\Delta t + d^{1/2}}{1 + 6\dot{q}_{1prev}^2\Delta t^2} \qquad (20)$$

$$d = (1 + 6\dot{q}_{1prev}^2\Delta t^2)(a^2 - \mathrm{g}^2)/a_1^2 - 2\dot{q}_{1prev}^6\Delta t^2 - \dot{q}_{1prev}^4$$

The previous equation is valid for the movement that has a positive acceleration onset. For the movement that has a negative acceleration onset, the discriminant d is mostly negative, which means that this equation cannot be used directly. In that case, a simple solution is used, in which the values of $\ddot{q}_1$ for the positive acceleration onset n of the same magnitude are reversed. Solving (17) for every interpolation period in the form of Jacobi elliptic integrals gives less precise solution [19].

B. Smoothing the acceleration force G profile

While a normal acceleration $a_n = a_1\dot{q}_1^2$ and gravity g act all of the time during the centrifuge movement, the tangential acceleration $a_t = a_1\ddot{q}_1$ does not act during the movement that has a constant load G. The transition from a varying to a constant acceleration causes an abrupt increase in $\dot{q}_1$, while the transition from a constant to a varying acceleration causes the abrupt decrease in $\dot{q}_1$. The abrupt change in $\dot{q}_1$ causes an abrupt change in q_2 (which can be seen from (11) and (12)) and a very large value of $\ddot{q}_1$, which causes an abrupt change in q_3; these relationships can be seen from (13) and (14). To prevent the abrupt change in $\dot{q}_1$, it is adopted that before and after the given linear change in G, i.e., acceleration a, there is a period of smoothing of the acceleration curve. The change in the acceleration has three different stages. Within the first period, smoothing is performed in such a way that the acceleration onset n changes linearly from 0 to a given value (jounce, or snap – the rate of change of the jerk with respect to time). Afterward, there is a period in which there is a constant acceleration rate. Within the third period, smoothing is performed in such a way that the acceleration onset n changes linearly to zero (snap). Thereafter, the total acceleration change is denoted by a_e - a_s, where a_s is the initial value of the acceleration, and a_e is the desired acceleration value. The percentage of the linear acceleration change part to the total acceleration change is denoted by c_{ac}. This part varies depending on the size of the absolute value of a_e - a_s. Here, c_{ac}=0.12 for $abs(a_e - a_s)$<1.59 g, and c_{ac}=0.8 for $abs(a_e - a_s)$>10.59 g. If 1.59 g<$abs(a_e - a_s)$<10.59 g, then c_{ac} changes linearly from 0.12 to 0.8. Within the smoothing algorithm, it is necessary to determine the following parameters: N_a, which is the number of interpolation periods in the starting or ending stage of the G load change; N_c, which is the number of interpolation periods for n_d=*const*; n, which is the desired acceleration rate of change after discretisation of (17) and ignoring the terms with Δt^3 and Δt^4; and Δn, which is the increase/decrease of n in one interpolation period at the starting or ending stage of the acceleration change. If we assign $sign(a_e - a_s)$=1 if a increases and $sign(a_e - a_s)$=-1 if a decreases, then these parameters will be calculated in the following way:

$$N_c = c_{ac}\,(a_e - a_s)/(n_d\ g\ \Delta t) \qquad (21)$$

$$N_a = sign(a_e - a_s)\,[(a_e - a_s)/(n_d\ g\ \Delta t) - sign(a_e - a_s)\,N_c] - 1 \qquad (22)$$

$$\Delta n = n_d / N_a \qquad (23)$$

$$n = \frac{sign(a_e - a_s)\,(a_e - a_s) - (N_a + N_c + 1)\,n_d\ g\ \Delta t}{(2N_a + N_c)\,g\,\Delta t} \qquad (24)$$

Even though the acceleration profile is smoothed, in transitions from a varying to a constant acceleration a (i.e., G and the angular velocity $\dot{q}_1$ of the centrifuge arm), in the first interpolation period after the transition, a small tangential acceleration appears. This appearance affects the acceleration load G, which has already been achieved. To nullify these effects, it is necessary to make a small correction in the angular velocity $\dot{q}_1$, which gives a new angular acceleration

$\ddot{q}_1 = (\dot{q}_1 - \dot{q}_{1prev})/\Delta t$ of axis 1. The motor of this axis can achieve a desired angular velocity $\dot{q}_1$ in one interpolation period. However, with regard that angle q_3, depends on $\ddot{q}_1$, (13) and (14), there could be an abrupt pitch rotation of the cockpit. To avoid this rotation, an algorithm is developed that yields a smooth approach to the given G load.

C. Control algorithm

First, N_c, N_a, Δn and n are calculated with (21), (22), (23) and (24), respectively. Then, the centrifuge kinematic parameters are calculated in three phases. For the positive acceleration onset in the first phase, the onset of the centrifuge inertial force (jerk =$\Delta a/\Delta t$) increases linearly from zero to the programmed value. In the second phase, this force increases linearly (n=const), and in the third stage, the onset of this force decreases linearly from the programmed value to zero. In the first and third phases, smoothing of the acceleration force profile is performed. For the deceleration motion, the smoothing is performed vice versa. These three phases of the centrifuge control algorithm are shown below.

First phase.

for i=1 to N_a {

$n = n + \Delta n$, $a = a_{prev} + \Delta a = a_{prev} + sign(a_e - a_s)\, n\, g\, \Delta t$;

Step 1. Calculation of $\ddot{q}_1$ by (20) for the positive acceleration onset or the reading of the array $\ddot{q}_1 = -array(\ddot{q}_1[2N_a + N_c - i])$ for the negative acceleration onset;

Step 2. Calculation of the desired and maximal possible value of $\ddot{q}_1$ and the modified values of $\dot{q}_1$ and q_1 (out of the scope of this paper);

Step 3. Calculation of q_2 by (11) or (12) and q_3 by (13) or (14), and $\dot{q}_i = (q_i - q_{iprev})/\Delta t$, $\ddot{q}_i = (\dot{q}_i - \dot{q}_{iprev})/\Delta t$, i =2,3;

Step 4. Calculation of the desired and maximal possible values of $\ddot{q}_2$ and $\ddot{q}_3$, and the corrected values for $\dot{q}_2$, q_2, $\dot{q}_3$ and q_3 (out of the scope of this paper);

$\dot{q}_i = \dot{q}_{iprev} + \ddot{q}_i\, \Delta t$, $q_i = q_{iprev} + \dot{q}_i\, \Delta t$, $\dot{q}_{iprev} = \dot{q}_i$, $q_{iprev} = q_i$, i =1, 2, 3. }

Second phase.

for i=1 to N_c {

$a = a_{prev} + \Delta a = a_{prev} + sign(a_e - a_s)\, n\, g\, \Delta t$;

Calculating $\ddot{q}_1$ by (20) for the positive acceleration onset or reading the array $\ddot{q}_1 = -series(\ddot{q}_1[N_a + N_c - i])$ for the negative acceleration onset; The remainder of this phase is the same as in the first phase.}

Third phase.

for i=1 to N_a {

$n = n - \Delta n$, $a = a_{prev} + \Delta a = a_{prev} + sign(a_e - a_s)\, n\, g\, \Delta t$;

Calculation of $\ddot{q}_1$ by (20) for the positive acceleration onset or reading of the array $\ddot{q}_1 = -series(\ddot{q}_1[N_a - i])$ for the negative acceleration onset;

The remainder of this phase is the same as in the first phase. Steps 2, 3 and 4 are the same as in the first phase.}

IV. Results: Verification for the Proposed Control Algorithm

The proposed control algorithm for the CFS motion was tested on the off-line programming system of the robot controller developed at the Lola Institute. G_z, G_x and G_y acceleration force profiles are provided by this programming system. Lola-Industrial Robot Language (L-IRL) is here extended with the GMOVE instruction and the additional parameters that are required for the centrifuge motion programming. The centrifuge movement control algorithm, presented above, is also added.

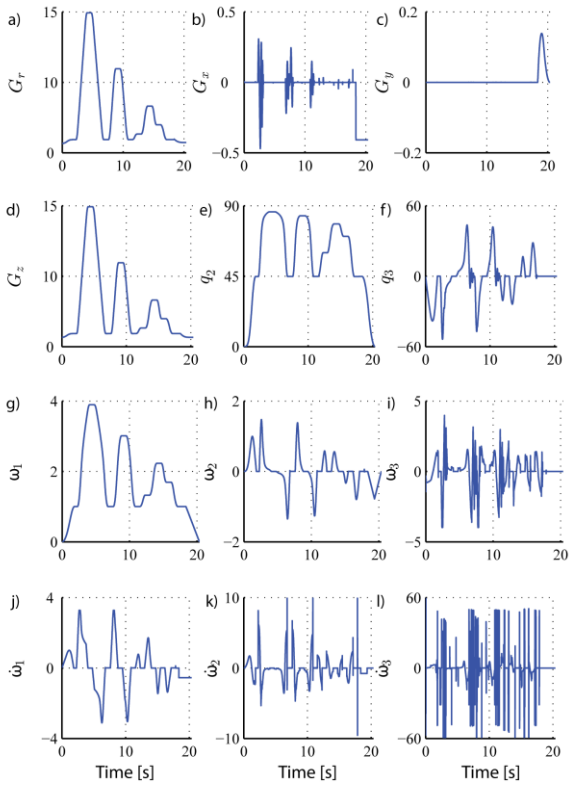

Fig. 5. Kinematic and dynamic parameters of the CFS motion of the program test 1: a) G_r =G, b) G_x, c) G_y, d) G_z [g], e) q_2=ϕ, f), q_3=θ [°] g) $\omega_1 = \dot{q}_1$, h) $\omega_2 = \dot{q}_2$, i) $\omega_3 = \dot{q}_3$ [s^{-1}], j) $\dot{\omega}_1 = \ddot{q}_1$, k) $\dot{\omega}_2 = \ddot{q}_2$, l) $\dot{\omega}_3 = \ddot{q}_3$ [s^{-2}].

Fig. 5 shows kinematic and dynamic parameters for an example of the centrifuge motion program. The masses, the mass centre coordinates and the principal moments of inertia about the link centres of mass in the link coordinate systems are given in the Appendix of this paper. In the commanded movement the desired transverse G_x and lateral G_y acceleration force components are equal to zero (G=G_z), and from a comparison of Figures 5a) and 5d) it can be concluded that this request is achieved. Herein, Figures 5 a), 5 b), 5 c) and 5 d) show G, G_x, G_y and G_z, respectively. It is shown that the centrifuge can achieve the mean growth of the acceleration

load of dG = 9 g/*s* in the period of constant acceleration change (c_{ac}) from the lower baseline level of G = 1.41 g to the upper baseline level of G = 15 g. The greatest absolute difference between the programmed and realised G_z change is 0.216 g. During the programmed motion, the deviation of G_x was between 0.38 and -0.5 g. There was no deviation in G_y. Based on that we can conclude that the calculation of the roll and pitch angles and presented control algorithm given in Section III are correct. After achieving G = 15 g, CMS sustains that acceleration force 0.7 s, and then decrease it with the offset of dG = -9 g/*s* till G = 1.41 g. Figures 5 a) and 5 d) depict the remainder of the program.

Figures 5 e) and 5 f) show the angles $q_2=\phi$ and $q_3=\theta$, which are obtained with the algorithm presented in subsection 4.4. Here, q_2 is between 0 and 86.2°, and q_3 is between 43.6 and -57.3°.

Figures 5 g), 5 h) and 5 i) show $\dot{q}_1$, $\dot{q}_2$ and $\dot{q}_3$. It can be observed that the presented algorithm limits the values for these velocities: $\dot{q}_1$ is not larger than 4.28 s^{-1}, $\dot{q}_2$ is between 1.47 and -1.35 s^{-1}, and $\dot{q}_3$ is between 3.98 and -3.98 s^{-1}.

Figures 5 j), 5 k) and 5 l) show $\ddot{q}_1$, $\ddot{q}_2$ and $\ddot{q}_3$. These values are also limited: $\ddot{q}_1$ is between 3.27 and -3.11 s^{-2}, $\ddot{q}_2$ is between 9.88 and -9.4, and $\ddot{q}_3$ is between 52.1 and -52.1 s^{-2}.

V. Conclusions

In this paper, a new centrifuge motion simulator for pilot training has been presented. This device is modelled as a manipulator that has three rotational axes. The centrifuge produces the desired transverse G_x, the lateral G_y and the longitudinal G_z acceleration forces and the roll, $\hat{\omega}_x$, pitch, $\hat{\omega}_y$ and yaw, $\hat{\omega}_z$ angular velocities, which simulate the acceleration forces and angular velocities that are accomplished by state-of-the-art aircraft.

The algorithm which generates the constant increase in the acceleration force acting on a pilot is given in this paper. To prevent the abrupt change in the arm angular velocity before and after the desired linear change in the acceleration force, smoothing of the acceleration force profile through arm motion is performed. The calculation of the roll and pitch angles of the gondola which have to direct the acceleration force into the desired direction is given as well.

Appendix

The masses, the mass centre coordinates and the principal moments of inertia about the link centres of mass in the link coordinate systems are: m_1=45500, m_2=1139, m_3=566 and m_4=250 kg, $\hat{\mathbf{r}}_1^{cm}=\left[-8.344\ -0.782\ 0.002\right]^T$, $\hat{\mathbf{r}}_2^{cm}=\left[0.\ 0.\ -0.004\right]^T$, $\hat{\mathbf{r}}_3^{cm}=\left[0.\ 0.\ 0.064\right]^T$ and $\hat{\mathbf{r}}_4^{cm}=\left[-0.5\ 0.005\ 0.55\right]^T$, $\hat{I}_{x1}$=91905, $\hat{I}_{y1}$=219978, $\hat{I}_{z1}$=243913, $\hat{I}_{x2}$=3243, $\hat{I}_{y2}$=1365, $\hat{I}_{z2}$=2010, $\hat{I}_{x3}=666$, $\hat{I}_{y3}=217$, $\hat{I}_{z3}=650$, $\hat{I}_{x4}=47$, $\hat{I}_{y4}=61$, $\hat{I}_{z4}=46$ kgm^2. The subscript $_4$ denotes here the external load.

Acknowledgment

This research is supported by the Ministry of Education, Science and Technological Development of Serbia under the project "Development of devices for pilot training and dynamic simulation of modern fighter planes flights: 3DoF centrifuge and 4DoF spatial disorientation trainer" (2011-2018), no. TR 35023.

References

[1] W. B. Albery, "Human Centrifuges: The Old and the New," In the Proceedings of the 36th Annual Symposium of the SAFE Association, Phoenix AZ, 14-16 September 1998.

[2] W. B. Albery, "Current and Future Trends in Human Centrifuge Development," SAFE Journal, 29, 2, September 1999.

[3] W. B. Albery, "Acceleration in Other Axes Affects +G_z Tolerance: Dynamic Centrifuge Simulation of Agile Flight," 75(1): 1-6, 2004.

[4] S. H. Schot, "Jerk: the time rate of change acceleration. American Journal of Physics," 46(11): 1090–4, 1978.

[5] J. Gallardo-Alvarado, "Jerk analysis of a six-degrees-of-freedom three-legged parallel manipulator," Robotics and Computer-Integrated Manufacturing, 28: 220–226, 2012.

[6] P. Morasso, "Spatial control arm movements. Experimental Brain Research," 42: 223–7, 1981.

[7] T. Flash, N. Hogan, "The coordination of arm movements: an experimentally confirmed mathematical model," Journal of Neuroscience, 5: 1688–703, 1985.

[8] Y. Uno, M. Kawato, R. Suzuki, "Formation and control of optimal trajectory in human multi joint arm movements. Biological Cybernetics," 61: 89–101, 1989.

[9] P. Viviani, R. Schneider, "A developmental study of the relationship between geometry and kinematics in drawing movements," Journal of Experimental Psychology: Human Perception and Performance, 17(1): 198–218, 1991.

[10] P. Viviani, T. Flash, "Minimum-jerk, two-third spower, law and isochrony: converging approaches to movement planning," Journal of Experimental Psychology: Human Perception and Performance, 21(1): 32–53, 1995.

[11] R. J. Crosbie, "Dynamic flight simulator control system," United States Patent, Number 4,751,662, Jun.14, 1988.

[12] R. J. Crosbie, D. A. Kiefer, "Controlling the Human Centrifuge as a Force and Motion Platform for the Dynamic Flight Simulator Technologies," Proceedings of the AIAA Flight Simulation Conference, St Louis, MO, AIAA Paper, 37-45, 1985.

[13] V. Kvrgic, J. Vidakovic, M. Lutovac, G. Ferenc, V. Cvijanovic, "A control algorithm for a centrifuge motion simulator," Robotics and Computer-Integrated Manufacturing, 30(4), pp. 399–412, 2014.

[14] V. Kvrgic, Z. Visnjic, V. Cvijanovic, D. Divnic, S. Mitrovic, "Dynamics and control of a spatial disorientation trainer," Robotics and Computer-Integrated Manufacturing, 35, pp. 104–125, 2015.

[15] M-H. Tsai, M-C. Shih, "*G*-load tracking control of a centrifuge driven by servo hydraulic systems," Proc. IMechE, Vol. 223, Part G: J. Aerospace Engineering, pp. 669-682, 2009.

[16] Y. C. Chen, D. W. Reperger, "A study of the kinematics dynamics and control algorithms for a centrifuge motion simulator," Mechatronics, Vol. 6, No. 7, pp. 829-852, 1996.

[17] Y. C. Chen, D. W. Reperger, Roberts R, "Study of the kinematics, dynamics and control algorithms for a centrifuge motion simulator," Proceedings of the American Control Conference, Vol. 3, pp. 1901-1905, 1995.

[18] M. Lutovac, V. Kvrgic, G. Ferenc, Z. Dimic, J. Vidakovic, „3D simulator for human centrifuge motion testing and verification," 2nd Mediterranean Conference on Embedded Computing MECO, pp. 160-163, 2013.

[19] J. Vidakovic, G. Ferenc, M. Lutovac, V. Kvrgic, „Development and implementation of an algorithm for calculating angular velocity of main arm of human centrifuge," 15th International Power Electronics and Motion Conference, EPE-ECCE 2012 Europe Congress, pp. DS2a.17, 2012.